

Influence of the Velocity of Plasma-Sprayed Particles on Splat Formation

S. Fantassi, M. Vardelle, A. Vardelle, and P. Fauchais

The behavior of individual plasma-sprayed particles as they impinge on a surface was monitored using two high-speed two-color pyrometers, one focused 2 mm before the substrate and the other focused on the substrate surface. The influence of the velocity of the impinging particles (determined from the time of flight between the two focused points of the pyrometers) on the deformation and cooling processes was investigated. Results on zirconia particles impacting on a smooth bare steel substrate are presented in terms of apparent flattening time, splat diameter, and cooling rate determined from the pyrometer signals.

1. Introduction

THE spreading kinetics of plasma-sprayed particles impinging on a substrate surface determines the shape and the thickness of the splats as well as the real area of contact between the flattened droplet and the substrate or previously deposited material. These contact areas depend on gas entrapment, contaminant inclusions, and the wetting characteristics at the impacting particle/surface interface. They influence coating cohesion and adhesion through parameters such as surface roughness (correlated to particle size), particle velocity and molten state on impact, and the temperature of the substrate or previously deposited layers (in connection with wettability).^[1]

The phenomena controlling the manner in which a molten or semimolten particle flattens and solidifies on impact are not yet completely understood. However, the effects of parameters such as droplet velocity and temperature have been stressed by different studies (see for example Ref 1 to 3). With the development of experimental devices that allow one to monitor particle spreading and cooling,^[4,5] the relationship between particle parameters on impact and the flattening process can be investigated.

In the present work, the influence of particle impact velocity on flattening time and flattening degree (which is defined as the ratio of the diameter of the resulting splat to the diameter of the impacting droplet) were studied while other parameters (molten state of the particles, nature, roughness and temperature of the surface) were kept constant. The measurement technique using two high-speed two-color pyrometers provides data on the temperature, the velocity and the size of a particle prior to its impact on a substrate, and on its flattening and cooling when it impinges on the substrate surface. Results on zirconia particles with velocities ranging from 100 to 300 m/s, plasma sprayed onto smooth steel substrates, are presented.

2. Measurement Technique

The in-flight surface temperature of a single particle and its thermal history on impact and cooling on the substrate were determined from measurements of the thermal radiation of this particle at two wavelengths. The measurement system consisted of two high-speed two-color pyrometers: one was focused 2 mm before the substrate and the other was focused on the substrate, as shown in Fig. 1.^[5] The light emitted by an incandescent particle in flight or on impact was collected and directed through optical fibers to the entrance slit of a monochromator. And two output signals, filtered at 632.8 and 832.8 nm, respectively, were transmitted to two photomultipliers.

After amplification, the signals were recorded by a numerical oscilloscope triggered by a coincidence signal when a particle was detected simultaneously by the first pyrometer and an optical sensor focused at the same point. The temperature of the in-flight particle was derived after calibration from the ratio of the two detector outputs, assuming the particle behaved as a grey body. The temperature evolution of the impacting particle was also computed from the ratio of the two detector outputs up to the time corresponding to a signal intensity equal to 10% of the maximum signal intensity. Then, the temperature evolution was computed from one detector output taking into account the evolution of material emissivity with temperature (generally known for the solid material). The spatial resolution for the in-flight measurement was approximately 0.015 mm³, and the monitored area on the substrate surface was about 0.25 mm².

The particle velocity was deduced from the time of flight between the two focusing points of the two pyrometers. The diameter, d , of the impacting particle and the diameter, D , of the resulting splat were determined after calibration, from the maximum signal intensity. This calibration used a tungsten arc lamp and consisted of recording the amplitude of signals in accordance with the emission surface.^[5] The experimental procedure and the information from such measurements are summarized in Fig. 2.

During the experiments, the velocities and surface temperatures of the particles passing through the first measuring volume were simultaneously measured by a system consisting of a laser doppler velocimeter (LDV)^[6] and a high-speed pyrometer.^[7] This measurement system presented statistical data on about 1000 particles and independently verified the data gained from

Key Words: diagnostics, flattening time, particle temperature, particle velocity, splat formation

S. Fantassi, M. Vardelle, A. Vardelle, and P. Fauchais, Laboratoire Matériaux Céramiques et Traitements de Surface, Equipe Plasma, Laser, Matériaux—URA CNRS 320, Université de Limoges—123, Avenue Albert Thomas, 87060 Limoges Cedex, France.

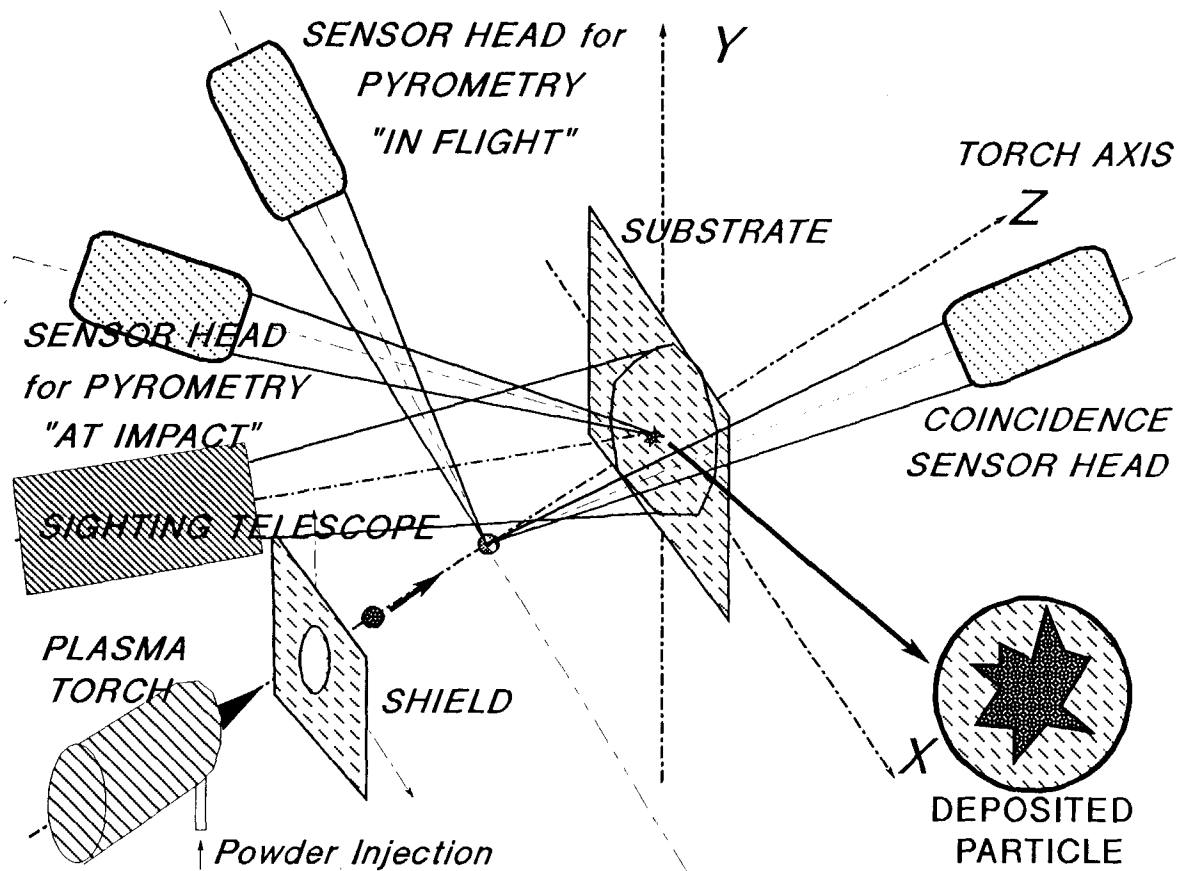


Fig. 1 Schematic of experimental setup with the two pyrometers and the coincidence sensor.

Table 1 Plasma spraying parameters with custom-built torch

Experiment No.	Nozzle diameter, mm	Plasma gas flow rate, L/min	Voltage, V	Arc current, A	Carrier gas flow rate, L/min	Particle mean velocity, m/s
1	10	45 Ar + 15 H ₂	65	600	3.0	105
2	6	32 Ar + 12 H ₂	60	600	2.8	190
3	7	75 Ar + 25 H ₂	68	600	6.5	230

the device shown in Fig. 1. The experimental arrangement shown in Fig. 1 sampled 50 to 100 events during any particular run.

3. Experimental Procedure

The material used in this investigation was yttria-stabilized zirconia (8 wt% Y₂O₃). The powder (fused and crushed, -45+22 µm) was injected radially 3 mm upstream of the nozzle exit at a low feeding rate (4 g/min). The internal diameter of the injector was 1.8 mm, and the carrier gas flow rate was adjusted according to torch operating conditions in such a way that the mean trajectory of the powder crossed the plasma jet axis with an angle of 4°. The spray distance was 12 cm. The monitored area on the substrate was selected by using a water-cooled screen made of stainless steel in which a 3-mm hole ensured that some particles

passed through to the substrate. The hole of the metal mask was positioned so that only particles following the mean trajectory were collected. This metal mask was protected from plasma heat flux by a second double-walled water-cooled screen that was moved by a pneumatic system. The screen was opened for a few seconds so that about 50 to 100 splat events were recorded.

The substrate consists of an array of five to ten rectangular steel targets (35 × 10 × 1 mm³) positioned in the same plane orthogonal to the jet axis. The steel sheet has a surface roughness of 0.4 µm. Once ten particle impacts have been recorded on a target, it is replaced by another new target so that only the flattening and cooling of particles sprayed on bare steel surface is studied.

The spraying was performed in air with an argon/hydrogen plasma-forming gas. Plasma spraying was carried out with three sets of parameters chosen to achieve different ranges of particle velocity at impact. The spraying parameters as well as the mean particle velocity measured by laser doppler velocimeter at the spraying distance of 12 cm are given in Table 1.

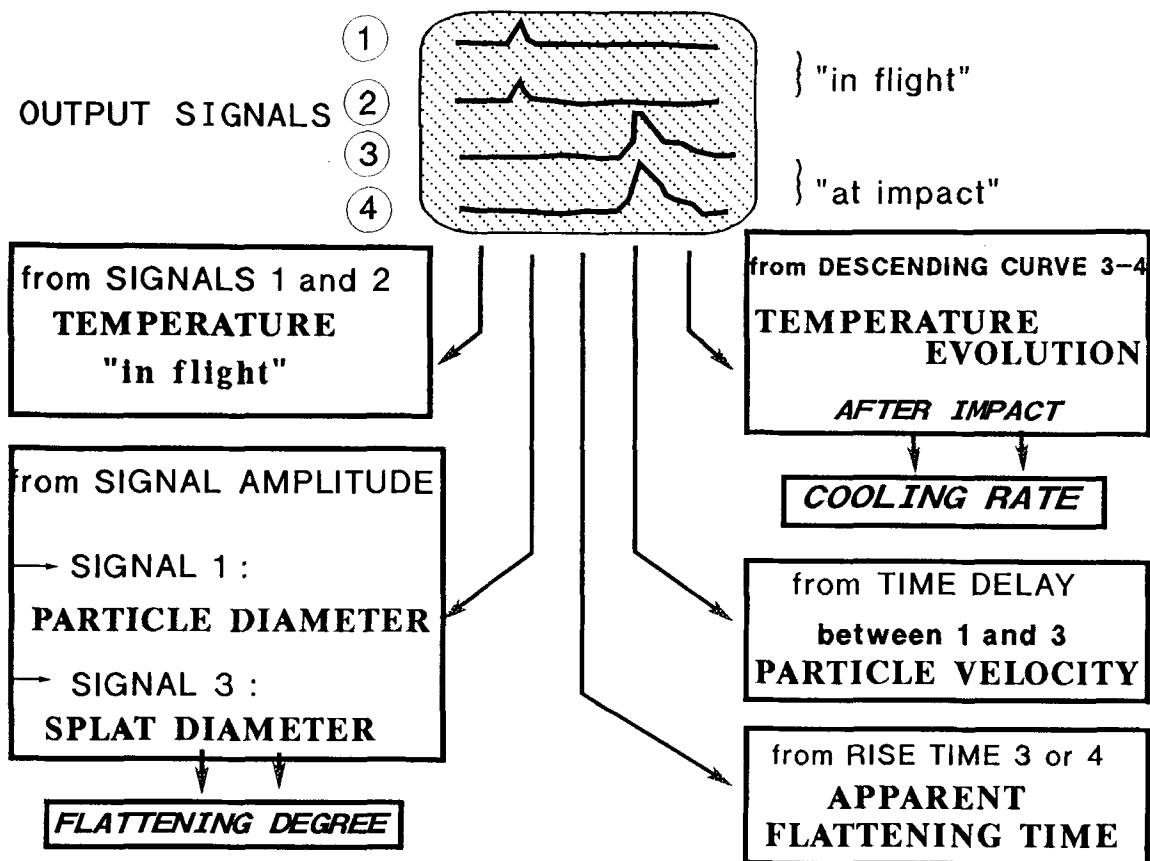


Fig. 2 Experimental procedure for monitoring particle behavior at impact.

4. Results and Discussion

4.1 Example of Signals Collected by Two Pyrometers

Figure 3 shows an example of signals (S1-S2) recorded when a particle crosses the first measuring volume and then impinges on the substrate (S3-S4). The evolution of the temperature of the splat (calculated from the ratio of the signals S3-S4) is also shown (by the symbols in the graph and the right axis) in Fig. 3. Light signals collected from the in-flight particle are one order of magnitude lower than the signals collected from the impinging particle. The shapes of the first and second pulses are also very different. The signals gained from the in-flight particle are almost symmetrical, with the particle crossing the measuring volume at a constant velocity. The rise of the detected radiation at impact is explained by an increase in the radiating surface when the particle spreads on the substrate. The signals coming from the flattening particle exhibit steep rises corresponding to a very short flattening time (a few microseconds). The maxima in signal intensities is followed by a delayed decrease, which corresponds to the cooling of the splat mainly by conduction to the substrate. The flattening time was determined from the rise time of the second pulse (S3-S4). Two mechanisms might account for the termination of droplet flattening on impact—these being a conversion of particle kinetic energy into surface and viscous energy and freezing rate. As shown by Moreau,^[8] the flattening duration computed from the rise time of the pulses

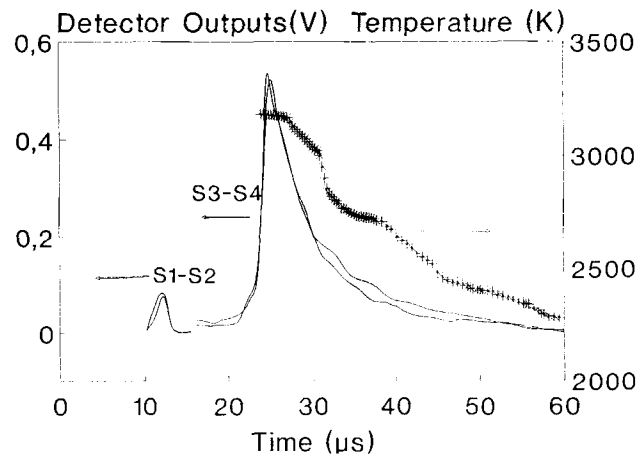


Fig. 3 Example of collected signals "in-flight" and "at impact" and the corresponding temperature curve during splat cooling.

corresponds to the real flattening time only if splat freezing intervenes after spreading is complete.

4.2 Distributions of Particle Parameters at Impact (Experiment 2)

Figures 4 to 6 illustrate typical results obtained from the second set of experimental conditions (see Table 1). The particle

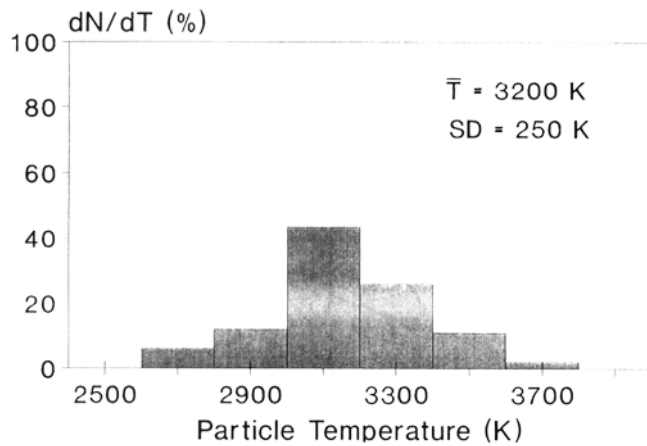
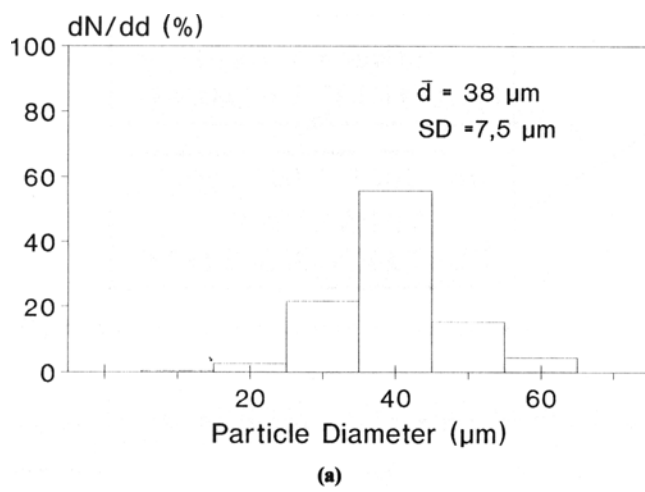
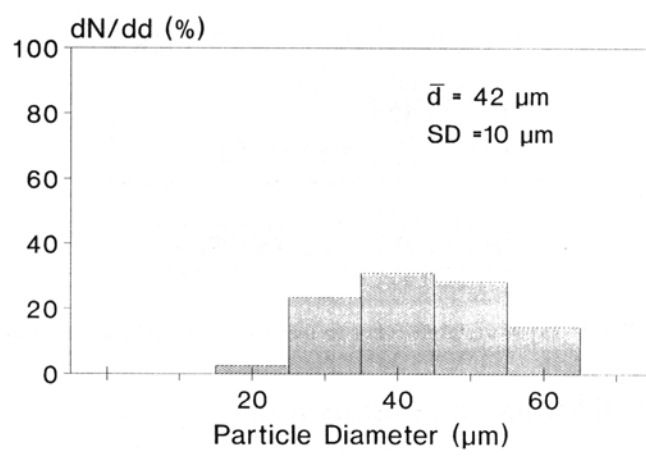


Fig. 4 Histogram of particle temperature prior to impact (Experiment 2). dN/dT is the percentage of the impacting particles, with temperature between T and $T + dT$ ($dT = 200 \text{ K}$); SD is the standard deviation of the temperature measurement value.

surface temperatures presented in Fig. 4 are close to the melting point of ZrO_2 (i.e., 2950 K). The size distributions of the zirconia powder received from the manufacturer and determined from the maximum of light pulses collected from the first measurement volume as previously explained are shown in Fig. 5(a) and (b). The mean values (38 and 42 μm , respectively) are in good agreement. However the in-flight size measuring method, based on the analysis of particle thermal radiation, promotes detection of large particles because the surface temperature range of the detected particles is rather narrow (3000 to 3500 K), and the smaller particles may cool below the detection limit in preference to the larger particles. The particle velocity distributions (given in Fig. 6a and b), determined by LDV and time of flight between the focusing points of the two pyrometers, are similar. The average velocity measured by the method indicated in Fig. 1 is lower (180 m/s instead of 190 m/s with the LDV technique) because this preferentially analyzes the large-diameter particles.

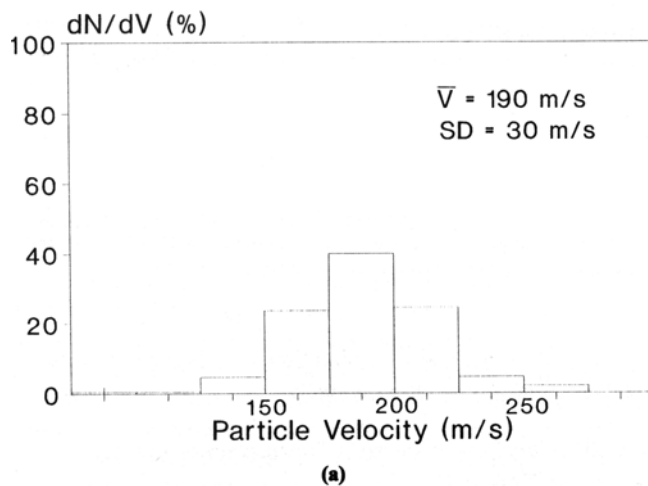


(a)

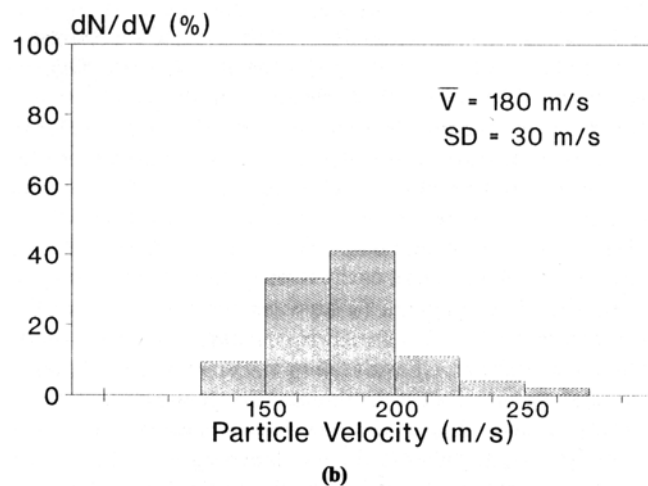


(b)

Fig. 5 (a) Histogram of the particle size as given by the manufacturer. dN/dd is the percentage of the impacting particles, with diameter between d and $d + dd$ ($dd = 10 \mu\text{m}$). (b) Histogram of the particle size on impact (Experiment 2).



(a)



(b)

Fig. 6 (a) Histogram of the particle velocity on impact measured by LDV (Experiment 2). dN/dV is the percentage of the impacting particles, with velocity between V and $V + dV$ ($dV = 25 \text{ m/s}$). (b) Histogram of the particle velocity on impact (Experiment 2).

4.3 Evolution of Flattening Time and Degree

The experimental results are represented in Fig. 7 to 9. These results are rather scattered, not only according to the distributions of particle size, temperature, and velocity at impact, but also to the different shapes of the resulting splats (from completely circular discs to disintegrated splats).

The dependence of the apparent flattening time on the particle velocity at impact is shown in Fig. 7. Flattening time varies from about 1.5 μ s when the velocity of the impinging particle is 100 m/s to about 0.7 μ s when the impact velocity is 300 m/s. Flattening time decreases with impact velocity, whereas it increases with the ratio of particle size to velocity, as illustrated in Fig. 8.

An analysis of spreading and cooling of droplets sprayed on cold surfaces has been reported by Madejski,^[9] who considered the effects of solidification kinetics on the spreading of droplets and predicted asymptotic values for the degree of flattening. In this approach, he considered a macroscopic balance for the radial flow of cylinders representing a spherical droplet of equal volume. He accounted for viscous flow and surface tension effects as well as a one-dimensional Stefan's approach to model the solidification problem. The work of Madejski showed that the degree of flattening can be expressed in terms of Reynolds, Weber, and Peclet numbers related to the particle and freezing

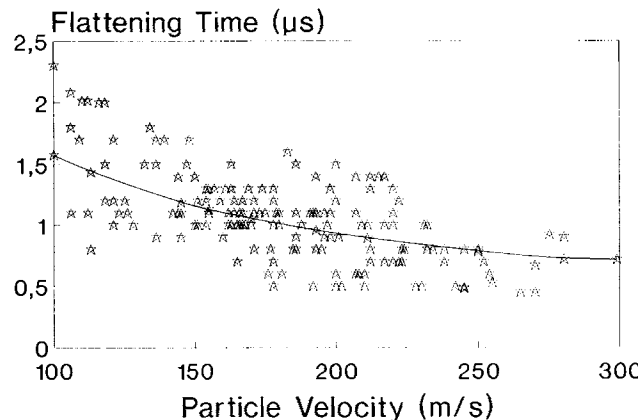


Fig. 7 Flattening time as a function of particle velocity.

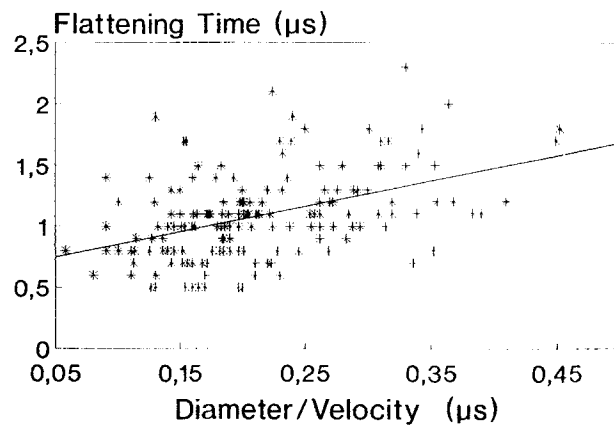


Fig. 8 Flattening time as a function of the ratio of particle size to velocity.

characteristics of the material. For plasma spraying conditions characterized by Weber and Reynolds numbers greater than 100, MacPherson^[1] showed that, if spreading is complete before solidification, the degree of flattening (D/d) can be calculated from Madejski's analysis using the simplified equation:

$$D/d = 1.2941 \text{ Re}^{0.2} \quad [1]$$

where Re (Reynolds number) = $\rho v d / \mu$; v is the impact velocity; ρ is the density of the material; and μ is dynamic viscosity.

More recently, Yoshida^[3] investigated the effects of viscosity, size, and velocity variations on the deformation process at impact by using a numerical algorithm to model the impact of alumina droplets, assuming a constant temperature of droplets during deformation. The results suggested that deformation phenomena could be summarized by the following formula:

$$D/d = 0.83 \text{ Re}^{0.2} \quad [2]$$

Similar results were obtained by Solonenko^[10] and also by Trapaga and Szekely.^[11] From a numerical representation of the time-dependent spreading process, Trapaga and Szekely have shown that the final splat diameter may be described by:

$$D = d \text{ Re}^{0.2} \quad [3]$$

and the spreading time, t_s , may be approximated by the expression:

$$t_s = \frac{2d}{3v} \text{ Re}^{0.2} \quad [4]$$

These correlations do not take into account the nature of the substrate surface and its roughness even though recent experiments^[8] have emphasized their influence on the flattening process.

The flattening degree deduced from approximately 100 events with respect to Reynolds number is plotted in Fig. 9. This figure also shows the evolution of the degree of flattening obtained from Eq 1 and 2. Note that due to the lack of data on liquid zirconia Reynolds numbers have been computed assuming constant values for zirconia viscosity ($\mu = 4.10^{-2} \text{ kg/m} \cdot \text{s}$) and density ($\rho = 5700 \text{ kg/m}^3$). Therefore, the curves in Fig. 9 do not indicate the influence of the particle molten state at impact, but reflect only the influence of particle size and velocity on the de-

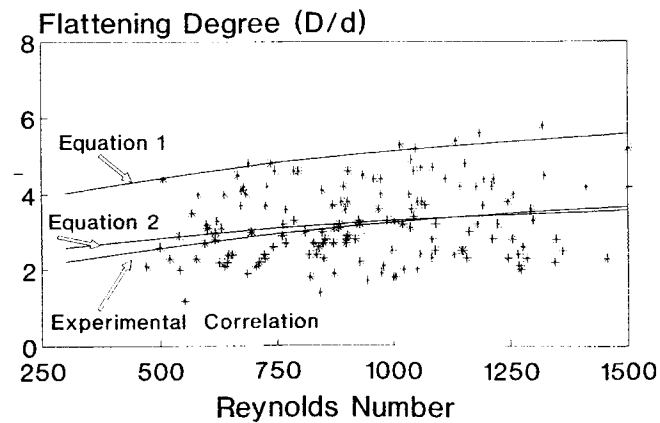


Fig. 9 Degree of flattening as a function of Reynolds number.

formation process. Although the experimental data are scattered, the correlation computed from the authors' experimental data approximately follows Eq 2.

The splat cooling rate depends on splat thickness, material thermal properties, and contact area between the splat and the substrate. The mean cooling rate was determined from the time required for the signals of the impinging particles to decrease by one order of magnitude from their maximum values. The results showed that the cooling rate slightly increases with the degree of flattening. The mean value is on the order of $100 \text{ K}/\mu\text{s}$. This high value may be explained by the high thermal conductivity of steel. Because the thermal conductivity of the zirconia splat is much lower, the cooling rate is controlled by the heat transfer coefficient between the splat and the substrate and is specified by the contact thermal resistance. An estimate of this transfer coefficient from the experimental mean cooling rate produces a value of about $4.10^5 \text{ W/m}^2 \cdot \text{K}$.

5. Conclusion

Investigations on particle/substrate interactions during the plasma spray process have been carried out using two high-speed pyrometers. This measurement system allows study of particle flattening and splat cooling as a function of particle parameters (size, velocity, and temperature) at impact.

This report is confined to the study of the effect of impact particle velocity on spreading and cooling processes on a smooth substrate kept at a temperature below 100°C . For zirconia particles sprayed on steel substrates, flattening time decreased with particle velocity, but increased with particle diameter. It was also found that the evolution of degree of flattening as a function of Reynolds number is consistent with the theoretical prediction of Yoshida.^[3] Moreover, the cooling rate was about $100 \text{ K}/\mu\text{s}$ for these specific experimental conditions.

To determine reliable correlations between flattening and cooling data and particle parameters at impact, it is necessary to perform experiments on materials whose thermodynamic and transport properties are known at high temperature (alumina or tungsten for example) and also to improve the measurement accuracy of the size of the particle in flight. This study would be useful to validate mathematical models of particle impingement during the spray process, to model coating growth, and to inter-

pret coating microstructure and adhesion/cohesion properties. Such work is now in progress.

Acknowledgments

This work was carried out under grant N°BREU/0418 from the Commission of the European Communities under the Brite-Euram Program. It is based on a presentation made at the National Thermal Spray Conference, Anaheim, CA, USA, 1993.

References

1. R. MacPherson, The Relationship Between the Mechanism of Formation, Microstructure and Properties of Plasma-Sprayed Coatings, *Thin Solid Films*, Vol 83, 1981, p 297-310
2. C.A. Williams and H. Jones, The Effect of Melt Superheat and Impact Velocity on Splat Thickness, *Mater. Sci. Eng.*, Vol 19, 1975, p 293-297
3. T. Yoshida, T. Okada, H. Hamatani, and H. Kumaoka, Integrated Fabrication Process for Solid Oxide Fuel Cells using Novel Plasma Spraying, *Plasma Sources Sci. Technol.*, Vol 1, 1992, p 195-201
4. C. Moreau, P. Cielo, M. Lamontagne, S. Dallaire, and M. Vardelle, Impacting Particle Temperature Monitoring during Plasma Spray Deposition, *Meas. Sci. Technol.*, Vol 1, 1990, p 807-814
5. M. Vardelle, A. Vardelle, P. Fauchais, and C. Moreau, Pyrometer System for Monitoring the Particle Impact on a Substrate During Plasma Spray Process, *J. Measurement Sci. Technol.*, accepted for publication
6. A. Vardelle, J.M. Baronnet, M. Vardelle, and P. Fauchais, Measurement of the Plasma and Condensed Particles Parameters, *IEEE Trans. Plasma Sci.*, Vol PS8, 1980, p 417-424
7. J. Mishin, M. Vardelle, J. Lesinski, and P. Fauchais, Two-Colour Pyrometer for the Statistical Measurement of the Surface Temperature of Particles under Thermal Plasma Conditions, *J. Phys. E Sci. Instrum.*, Vol 20, 1987, p 620-625
8. C. Moreau, P. Cielo, and M. Lamontagne, Flattening and Solidification of Thermally Sprayed Particles, *J. Thermal Spray Technol.*, Vol 1, 1992, p 317-323
9. J. Madejski, Solidification of Droplets on a Cold Surface, *Int. J. Heat Mass Transfer*, Vol 19, 1976, p 1009-1013
10. O.P. Solonenko, M. Ushio, and A. Ohmari, Comprehensive Investigation of Metal Drop-Substrate Interaction, *Thermal Spray Coatings: Research, Design and Applications*, C.C. Berndt and T.F. Bernecki, Ed., ASM International, 1993, p 55-60
11. G. Trapaga and J. Szekely, Mathematical Modeling of the Isothermal Impingement of Liquid Droplets in Spraying Processes, *Metall. Trans. B*, Vol 22, 1991, p 901-914